Substrates Matter: Influence of an Adjacent Dielectric on an Individual Plasmonic Nanoparticle

ARTICLE *in* NANO LETTERS · MAY 2009

Impact Factor: 13.59 · DOI: 10.1021/nl900945q · Source: PubMed

5 AUTHORS, INCLUDING:

Mark W. Knight
FOM Institute AMOLF
30 PUBLICATIONS **2,104** CITATIONS
SEE PROFILE

Naomi J Halas
Rice University
329 PUBLICATIONS **35,584** CITATIONS
SEE PROFILE

NANO LETTERS

2009
Vol. 9, No. 5
2188-2192

Substrates Matter: Influence of an Adjacent Dielectric on an Individual Plasmonic Nanoparticle

Mark W. Knight,[†,‡] Yanpeng Wu,[‡,§] J. Britt Lassiter,[‡,§] Peter Nordlander,[*,‡,§] and Naomi J. Halas[*,†,‡,§,||]

Department of Electrical and Computer Engineering, Department of Chemistry, Department of Physics and Astronomy, and the Laboratory for Nanophotonics, Rice University, 6100 Main Street, Houston, Texas 77005

Received March 25, 2009; Revised Manuscript Received March 31, 2009

ABSTRACT

Studying the plasmonic properties of metallic nanoparticles at the individual nanostructure level is critical to our understanding of nanoscale metallic systems. Here we show how the presence of a nearby dielectric substrate modifies the energies of the plasmon modes of a metallic nanoparticle. The adjacent dielectric lifts the degeneracy of the dipole plasmon modes oriented parallel and perpendicular to the substrate, introducing a significant energy splitting that depends strongly on the permittivity of the substrate. This energy splitting can easily be misinterpreted as an anomalously broadened plasmon line shape for excitation of an individual nanoparticle with unpolarized light.

Metallic nanoparticles with their collective electronic resonances (surface plasmons) form a broad family of nanostructures of increasing variety, complexity, and technological importance. Plasmonic nanoparticles exhibit a remarkable sensitivity to their environment, where interactions with proximal structures and materials typically influence their plasmon properties in dramatic and easily observable ways. The interaction of plasmons on adjacent nanoparticles or the coupling of two plasmons on the same nanoparticle provide practical routes to the rational design of nanostructures with new plasmonic properties.[1,2] The influence of a directly adjacent[3] or an isotropically surrounding dielectric medium[4] also alters the plasmonic properties of a nanoparticle.[5,6] This effect has been of tremendous interest in the development of ultrasensitive localized surface plasmon resonant (LSPR) nanosensors capable of ultimately detecting individual molecular binding events.[7,8] In fact, the ease with which the properties of localized nanoparticle plasmons are influenced by their local environment has made definitive measurements of their fundamental characteristics a significant, ongoing challenge. As a result, the study of plasmonic nanoparticles at the individual nanostructure level has become a major experimental focus and has enabled numerous significant advances in our understanding of plasmons in nanoscale systems.[9] For example, in dark-field microspectroscopy, individual nanoparticles are dispersed onto a dielectric substrate, where UV−visible spectroscopy is subsequently performed on a nanostructure. Combining these local optical measurements with precise, nanoscale imaging of the individual nanostructure (e.g., scanning electron microscopy) allows us to relate the plasmonic properties of specific individual nanoparticles and their complexes to their specific nanoscale geometry. This enables quantitative comparison between the experimental spectra and theoretical calculations of their electromagnetic modes.

Given the success of this experimental approach, it is very important to examine the effect of the dielectric substrate on the plasmonic properties of the nanoparticle on its surface. The dielectric substrate provides a mechanism for symmetry-breaking, which has been shown in other plasmonic systems to lift mode degeneracies and modify the coupling of the plasmon modes to the far field.[10,11] It has been well established that the interaction between a plasmonic nanoparticle and adjacent metallic substrates of various geometries creates a strongly coupled plasmonic system, with hybridization of the localized surface plasmons of the nanoparticle and the propagating surface plasmon polaritons of the extended metal analogous to the Anderson model in condensed matter systems.[12−19] For an adjacent dielectric, this interaction is weaker with the nanoparticle plasmon coupling only to its image of surface charges, screened by the factor $(\varepsilon - 1)/(\varepsilon + 1)$ where ε is the permittivity of the substrate.[20] While the image dipole approximation is well known,[6] this

* To whom correspondence should be addressed. E-mail: (N.J.H.) halas@rice.edu; (P.N.) nordland@rice.edu.
[†] Department of Electrical and Computer Engineering.
[‡] Laboratory for Nanophotonics.
[§] Department of Physics and Astronomy.
[||] Department of Chemistry.

10.1021/nl900945q CCC: $40.75
Published on Web 04/10/2009

interaction is frequently neglected, or modeled as an effective refractive index embedding the nanostructure, altogether suppressing the reduced symmetry of the geometry.[21] Several approximate Mie scattering solutions have been developed to incorporate the effects of image multipoles for this geometry.[22−25] Computational models capable of incorporating substrate effects and asymmetric particle geometries have also been developed based on the discrete sources method (DSM),[26] the boundary element method (BEM),[6] and the discrete dipole approximation (DDA).[27]

Here we show how the properties of an adjacent dielectric slab substrate affect the plasmon modes of a spherical plasmonic nanoparticle, using polarization-dependent, dark-field microspectroscopy measurements of individual nanoparticles deposited on its surface. By examining the spectra of individual nanoparticles on substrates of varying permittivity, we observe that the dielectric substrate can exert a significant influence on the nanoparticle spectrum. While a spherical nanoparticle in an isotropic three-dimensional (3D) environment has three degenerate dipolar resonances, the reduced symmetry induced by the presence of the dielectric results in a splitting of these modes into two distinct resonances, corresponding to the nanoparticle dipole oscillating parallel and perpendicular to the substrate. For p-polarized light excitation, where coupling to the substrate is the strongest, a hybridized quadrupolar nanoparticle resonance can also be observed. These changes in mode properties are most clearly observable in the spectrum of a plasmonic nanoparticle on a high permittivity substrate (ZnSe). On lower permittivity substrates of more widespread use in single nanoparticle spectroscopy, such as silica glass, the mode splitting appears as an anomalous, "spoof" broadening of the plasmon mode resulting from p-polarized excitation of the nanoparticle−substrate system.

The following two types of plasmonic nanoparticles were used in these studies: Au/silica nanoshells, fabricated as previously reported,[28,29] and Au nanospheres (Ted Pella, Inc.). Both particle types were rinsed three times via centrifugation and resuspended in Milli-Q water (Millipore) prior to deposition on one of following three optical grade dielectric substrates: cleaned glass coverslips, uncoated sapphire windows (Edmund Optics), and uncoated ZnSe windows (II−VI Infrared). All substrates were prepared with alignment marks evaporated through transmission electron microscopy (TEM) grids to allow the direct comparison of single particle optical spectra and geometry.[30] Particles were deposited on substrates by spin-casting a dilute suspension of particles onto a substrate without an adhesion layer, resulting in sparse nanoparticle coverage.

The dark-field microscopy geometry allows light at an oblique angle to be incident on an individual nanoparticle, where light scattered by the nanoparticle is collected in a broad cone of solid angles defined by the numerical aperture of the microscope objective (Figure 1a). The dark-field microspectroscope employed for these experiments has been previously described.[10,30,31] Briefly, isolated particles were located on a gridded substrate using an inverted optical microscope (Zeiss Axiovert 200 MAT) using white light and

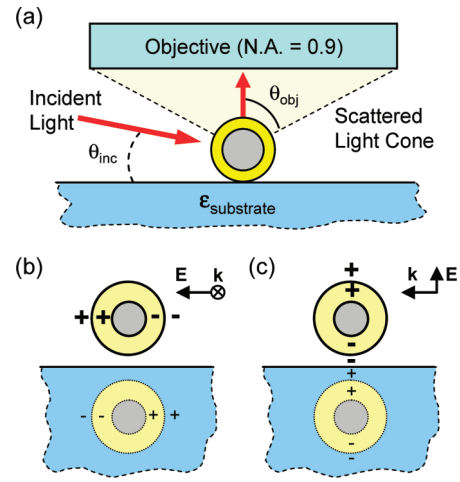

Figure 1. (a) Schematic of the optical system (not to scale) with a dark-field objective gathering the light scattered from an individual nanoparticle on a dielectric substrate. (b) Dipolar charge distribution for p-polarized incident light and (c) s-polarized incident light.

a 100×, 0.9 NA dark-field objective. Spectra were acquired by focusing the particle image on the entrance slit of a spectrometer (Acton Microspec 2150i) and recording the image on a thermoelectrically cooled CCD (Princeton Instruments, PhotonMax 512). The spectral efficiency, calibration, and background were accounted for in postprocessing using spectra of a broadband calibration standard source (Edmund Optics) and line filters.[31] Both p-polarized and s-polarized light were obtained by rotating a linear polarizer (LPVIS 100, Thorlabs) with respect to a wedge-shaped cutout in the optical path just after the halogen lamp. This wedge of light is then reflected off a single region of the darkfield objective mirror (Zeiss, 100×, 0.9 NA), and its polarization is maintained at the sample plane. Following optical characterization, the morphology of each nanoparticle studied was characterized using low vacuum scanning electron microscopy (ESEM, FEI Quanta 400). The low pressure H_2O environment (∼0.98 Torr) allows surface charge to dissipate while viewing particles on dielectric substrates without the need for depositing a conductive layer on the experimental samples.

Theoretical spectra for nanoshells and colloid supported on an infinite film were calculated numerically using a commercially available FEM package (COMSOL Multiphysics 3.4 with the RF module).[11] The nanoparticles were modeled as concentric spheres of radii r_1 and r_2, and separated from the substrate by a gap of 1 nm. For this geometry, calculated spectra were consistent with experimentally observed spectra. The Au nanoshells were modeled using empirically determined bulk dielectric values with linear interpolation;[32] cores were set as Au for colloid, and silica ($\varepsilon = 2.04$) for nanoshells. The spherical simulation space was subdivided into two halves, air ($\varepsilon_{air} = 1$) and a variable permittivity substrate (ε_{subs}), each surrounded by an absorbing perfectly matched layer (PML). The substrate was modeled using constant permittivities for glass slides ($\varepsilon_{subs} = 2.31$), sapphire ($\varepsilon_{subs} = 3.13$), and ZnSe ($\varepsilon_{subs} = 7.13$). A realistic dielectric function for ZnSe, which varies from $\varepsilon =$

7.5−6.2 over the experimental spectral range of λ = 500−1000 nm),[33] was also used but found to have a negligible effect on the calculated spectra. When performing numerical simulations of this coupled system, a two-step solution process was used to avoid spectral artifacts from waves scattered by the boundary between the air PML and the substrate PML. First, the total field was determined numerically without the particle for a plane wave incident at an angle θ_{inc} (Figure 1a), then that field was inserted as the excitation field for the nanoparticle. In the scattered field formulation, this method results in low field intensities far from the nanoparticle. Spectra were calculated by integrating the far field determined using the Stratton−Chu formula[34] over a spherical boundary with an opening half angle of $\sin^{-1}$ (N.A.) to include the effect of a realistic microscope objective in air.

The plasmonic properties of the nanoparticle-dielectric system can be understood using the plasmon hybridization concept.[1,31] In contrast to the case of a nanoparticle near a metallic surface, on a dielectric surface there are no substrate plasmon resonances and therefore no direct interaction between the plasmon resonances of the particle and the surface leading to surface-hybridized plasmon modes.[12,14] For nanoparticles above a dielectric substrate, the influence of the substrate manifests itself only through the screening of the electromagnetic fields that provides the restoring force in the plasmon oscillation. The electromagnetic fields across a nanoparticle near a dielectric surface are different than for a nanoparticle in an isotropic environment. Substrate-induced changes can be understood qualitatively using a simple image picture (Figure 1b,c). The screening introduced by the dielectric surface is equivalent to the potential generated by a nanoparticle image with its image charges reduced by a factor of $(\varepsilon - 1)/(\varepsilon + 1)$.[20] Dielectrics with a larger permittivity will give rise to a stronger "image" and larger interactions. The spectral shifts resulting from the presence of an adjacent dielectric can simply be viewed as an interaction of the nanoparticle with its image with a strength determined by the nanoparticle−substrate separation, substrate permittivity, and polarization of incident light. Incident light polarized parallel to the substrate (s-polarization) will localize the charges further from the substrate surface, resulting in much weaker nanoparticle−substrate interactions (Figure 1b) than p-polarized excitation, which will give rise to a more strongly shifted plasmon mode energy (Figure 1c). For both polarizations, the substrate-induced screening field will be nonuniform across the nanoparticle and contain higher order multipolar components in the coordinate system centered on the nanoparticle. This nonuniform field will therefore induce a hybridization of the multipolar plasmon modes of the nanoparticle, and specifically, a mixing of the dipolar components with the higher order multipolar nanoshell plasmon resonances. This hybridization can thus render the dark quadrupolar and higher order multipolar modes excitable and visible in the spectrum of an individual nanoparticle.

Spectra of individual nanoshells on glass, sapphire, and ZnSe substrates were obtained for both s-polarized and p-polarized incident light excitation and compared with FEM

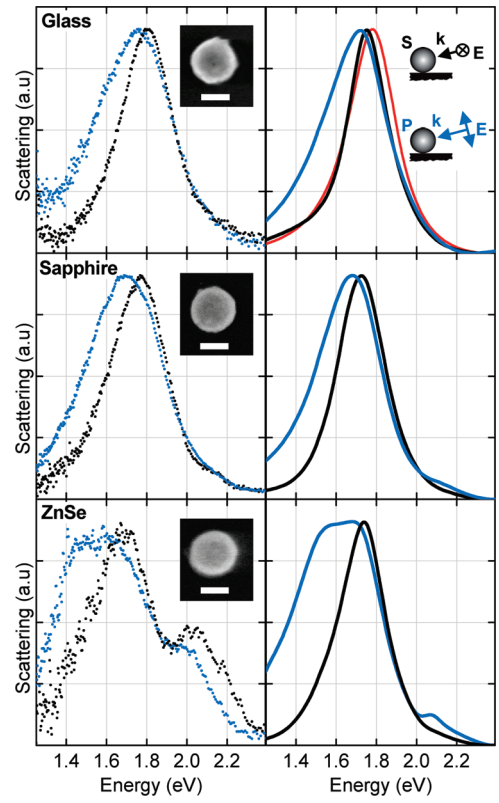

Figure 2. Comparison of experimental (left column) and theoretical calculations (right column) for nanoshells on glass (n = 1.52), sapphire (n = 1.77), and ZnSe (n = 2.67). Incident light was p-polarized (blue) or s-polarized (black) and incident at 79 ± 2°. Theoretical spectra correspond to an [r_1, r_2] = [67.0, 79.5] nm nanoshell calculated 1 nm above the substrate using polarized light incident at 79° with NA = 0.9. The red curve is Mie theory for the same nanoshell in an isotropic medium (air). Scale bars are 100 nm.

calculations of each system (Figure 2). On a glass substrate, a relatively small difference is observed in peak energies between s-polarized and p-polarized light. However, the line width of the p-polarized spectrum is increased dramatically relative to the s-polarized spectrum. We also show that the s-polarized spectrum on glass gives a spectrum nearly identical to the result obtained from Mie theory for the same nanoparticle in vacuum. This suggests that one can experimentally approximate the vacuum behavior of a nanoparticle by supporting the particle on a low-index substrate and using only s-polarized light excitation.

Increasing the substrate permittivity increases the mode splitting observed in the s- and p- polarized spectra (Figure 2). The broader peaks observed for p-polarized incident light are due to the simultaneous excitation of modes associated with polarizations parallel and perpendicular to the substrate. For the objective used, the polarized light was incident on the sample at an angle of 79 ± 2°. For s-polarized light, this allows an almost pure polarization parallel to the substrate surface; for p-polarized light, this includes components polarized both perpendicular and parallel to the substrate. Despite the large perpendicularly polarized component of the p-polarized incident light, the associated nanoparticle spectra all have a significant parallel (s-like)

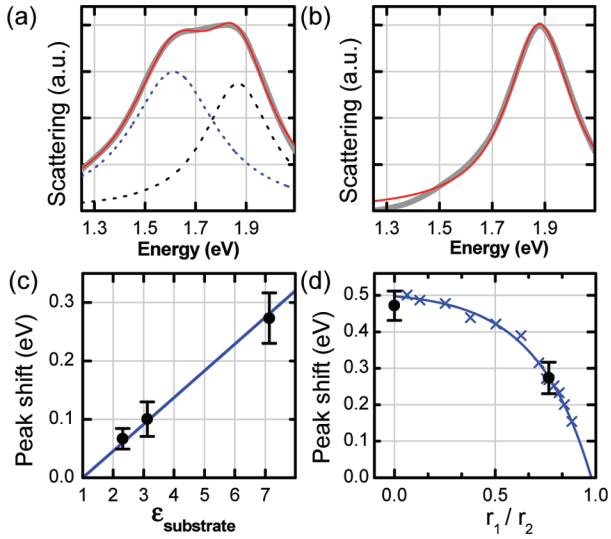

Figure 3. Linear dependence of substrate-induced plasmon mode splitting on substrate permittivity. (a) P-polarized spectrum calculated for an $[r_1, r_2] = [61.0, 79.5]$ nm nanoshell, with a 0.9 NA objective, and a bi-Lorentzian fit (red line). Lorentzian components are indicated by dotted lines. (b) S-polarized spectrum with a Lorentzian fit (red line). (c) Mean values of experimentally observed shifts from s to p peaks for nanoshells (black dots) with error bars indicating the standard deviation of the measurements. Theory fit (blue line) is for a [61.0, 79.5] nm nanoshell. (d) Theoretical s-to-p peak shifts (blue crosses) calculated on a ZnSe substrate for nanoshells with a 79.5 nm outer radius and varying inner radius. Calculated points are fit with an exponential (blue curve). Experimentally observed shifts are included for Au nanospheres and nanoshells (black points).

component, since the radiation pattern associated with the parallel mode preferentially scatters into the objective.[6]

For p-polarization to the ZnSe substrate, the interaction with the ZnSe surface is sufficiently strong that the quadrupolar nanoshell mode around 2.1 eV also shows up in the scattering spectrum. As mentioned above, this is caused by the inhomogenous electromagnetic field induced by the substrate. The electromagnetic field induced by the image of a real dipolar nanoparticle plasmon will have a quadrupolar component across the nanoparticle. Similarly, the field from the image of a real quadrupolar nanoparticle plasmon will have a dipolar component across the nanoparticle. The substrate-induced electromagnetic field thus couples the nanoparticle dipolar and quadrupolar plasmons and results in hybridized nanoparticle plasmons of finite dipole moments.

The calculated FEM spectra agrees very well with the experimentally measured spectra for both s- and p-polarizations and for the three different substrates. The slight discrepancies between theory and experiment are most likely due to slight structural deviations from a perfectly spherical nanoshell and perfectly smooth planar substrates in our experimental sample.

The s-polarized spectra obtained have a Lorentzian line shape, and the p-polarized spectra have a bi-Lorentzian line shape (Figure 3a,b). The bi-Lorentzian line shape of the p-polarized and, by extension, unpolarized spectra describes the apparent line width broadening observed experimentally. This superposition of two closely spaced Lorentzian curves

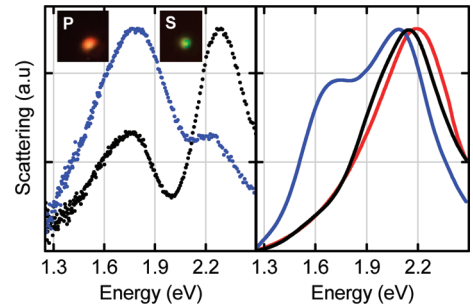

Figure 4. Comparison of experimental (left column) and calculated (right column) spectra for 154 nm diameter Au colloid on ZnSe ($n = 2.67$). Incident light was either p-polarized (blue) or s-polarized (black) and incident at 79°. Insets show optical images of the particle for s- and p-polarized light. Theoretical curve is for a 154 nm diameter colloid 1 nm above the substrate using polarized light incident at 79°. The red curve is Mie theory in an isotropic medium (air).

appears as a single broadened peak with a larger fwhm than predicted using computational or analytical solutions in air or using effective medium theory. Spectral analysis of individual nanoparticles on sapphire and ZnSe substrates reveals that the difference between the perpendicular and parallel mode energies increases linearly with substrate permittivity (Figure 3c). For each substrate, the average of the peak splitting energies observed, along with the associated standard deviation of our measurements, is shown. The resulting linear increase agrees closely with calculations using inner and outer radii of $[r_1, r_2] = [61.0, 79.5]$ nm, where the peaks are split by 45.8 meV/unit permittivity.

Increasing the peak splitting energy can also be accomplished by decreasing the nanoshell core−shell ratio (Figure 3d). Calculations for a range of nanoshells with different core radii and a shell radius of 79.5 nm show the largest shift for solid Au nanospheres, with decreasing shifts as the shell becomes progressively thinner. On ZnSe, this trend is well described by the exponential $\delta E = \delta E_{colloid} - Ae^{(r_1/r_2)/\tau}$, with $\delta E_{colloid} = 513$ meV, $A = 15$ meV, and $\tau = 0.276$. The magnitude of the calculated shifts of the perpendicular dipolar plasmon resonance are nominally half the magnitude of the shifts that would result from embedding the nanoparticle in a uniform dielectric of the same permittivity. This is consistent with only one side of the nanoparticle experiencing substrate-induced dielectric screening.

Given the observed linear dependence of the plasmon mode shift as a function of substrate permittivity, these results correspond to a splitting energy with a sensitive dependence on nanoparticle geometry, especially in the thin nanoshell regime. Experimental results are shown for Au nanospheres ($r_1/r_2 = 0$) and nanoshells ($r_1/r_2 = 0.763$), where error bars indicate the standard deviation of the measurements.

On the basis of this analysis, substrate-induced plasmon mode splitting should be most dramatic for solid Au nanospheres on ZnSe. This large shift, which clearly shows the existence of two plasmon modes in the p-polarized spectrum, is shown in Figure 4. The large split in energy between the perpendicular and parallel modes ($\delta E = 0.47$

± 0.04 eV) results in a visible, polarization-dependent change in color (Figure 4, insets). Similarly large spectral shifts and donut-shaped images associated with the p-polarized image have been reported for Au colloid over a gold film.[13]

In conclusion, we have shown that the presence of a dielectric substrate beneath an individual plasmonic nanoparticle can strongly influence its plasmon modes, causing the degenerate dipolar peak to split into two distinct modes corresponding to the dipoles oscillating parallel or perpendicular to the surface. These modes can be probed separately using s- or p-polarized incident light. For unpolarized incident light, both modes will be excited, resulting in an anomalously broad plasmon line width due to the mode splitting, rather than the intrinsic lifetime of the modes. The splitting between the perpendicular and parallel mode is found to increase linearly with increasing substrate permittivity, and is strongest for solid Au nanospheres. The finding of a strong substrate-induced anisotropy of the plasmon resonances of nanoshells deposited on a dielectric surface is expected to apply quite generally to other geometries and types of metallic nanoparticles. This effect needs to be considered when using spectra from individual nanoparticles on substrates to deduce plasmon energies and linewidths of individual nanoparticle plasmon modes.

Acknowledgment. We thank Britain Willingham and Yaroslav A. Urzhumov for insightful discussions on this subject, Bruce Brinson's assistance in nanoshell synthesis, and Jason H. Hafner's generosity in the use of his darkfield microscope. This work was supported by the Department of Defense Multidisciplinary University Research Initiative (MURI) W911NF-04-01-0203, the NSF IGERT Fellowship of M.W.K. (DG-0504425), the Robert A. Welch Foundation under Grants C-1222 (P.N.) and C-1220 (N.J.H.), and the Shared University Grid at Rice funded by the NSF under Grant EIA-0216467.

References

(1) Prodan, E.; Radloff, C.; Halas, N. J.; Nordlander, P. *Science* **2003**, *302*, 419–422.
(2) Wang, H.; Brandl, D. W.; Nordlander, P.; Halas, N. J. *Acc. Chem. Res.* **2007**, *40*, 53–62.
(3) Sherry, L. J.; Chang, S. H.; Schatz, G. C.; Van Duyne, R. P.; Wiley, B. J.; Xia, Y. *Nano Lett.* **2005**, *5*, 2034–2038.
(4) Tam, F.; Moran, C. E.; Halas, N. J. *J. Phys. Chem. B* **2004**, *108*, 17290–17294.
(5) Dmitriev, A.; Hägglund, C.; Chen, S.; Fredriksson, H.; Pakizeh, T.; Käll, M.; Sutherland, D. S. *Nano Lett.* **2008**, *8*, 3893–3898.
(6) Myroshnychenko, V.; Rodrı´guez-Fernández, J.; Pastoriza-Santos, I.; Funston, A. M.; Novo, C.; Mulvaney, P.; Liz-Marzán, L. M.; Garcı´a; de Abajo, F. J. *Chem. Soc. Rev.* **2008**, *37*, 1792–1805.
(7) Sannomiya, T.; Hafner, C.; Voros, J. *Nano Lett.* **2008**, *8*, 3450–3455.
(8) Mayer, K. M.; Lee, S.; Liao, H.; Rostro, B. C.; Fuentes, A.; Scully, P. T.; Nehl, C. L.; Hafner, J. H. *ACS Nano* **2008**, *2*, 687–692.
(9) Sonnichsen, C.; Franzl, T.; Wilk, T.; von Plessen, G.; Feldmann, J.; Wilson, O.; Mulvaney, P. *Phys. Rev. Lett.* **2002**, *88*, 177402.
(10) Wang, H.; Wu, Y.; Lassiter, J. B.; Nehl, C. L.; Hafner, J. H.; Nordlander, P.; Halas, N. J. *Proc. Natl. Acad. Sci. U.S.A.* **2006**, *103*, 10856–10860.
(11) Knight, M. W.; Halas, N. J. *New J. Phys.* **2008**, *10*, 105006.
(12) Nordlander, P.; Prodan, E. *Nano Lett.* **2004**, *4*, 2209–2213.
(13) Mock, J. J.; Hill, R. T.; Degiron, A.; Zauscher, S.; Chilkoti, A.; Smith, D. R. *Nano Lett.* **2008**, *8*, 2245–2252.
(14) Le, F.; Lwin, N. Z.; Steele, J. M.; Käll, M.; Halas, N. J.; Nordlander, P. *Nano Lett.* **2005**, *5*, 2009–2013.
(15) Lévêque, G.; Martin, O. J. F. *Opt. Express* **2006**, *14*, 9971–9981.
(16) Rueda, A.; Stemmler, M.; Bauer, R.; Mullen, K.; Vogel, Y.; Kreiter, M. *New J. Phys.* **2008**, *10*, 113001.
(17) Rueda, A.; Stemmler, M.; Bauer, R.; Vogel, Y.; Mullen, K.; Kreiter, M. *J. Phys. Chem. C* **2008**, *112*, 14801–14811.
(18) Park, W. H.; Ahn, S. H.; Kim, Z. H. *ChemPhysChem* **2008**, *9*, 2491–2494.
(19) Chu, Y.; Crozier, K. B. *Opt. Lett.* **2009**, *34*, 244–246.
(20) Novotny, L.; Hecht, B. *Principles of Nano-Optics*; University Press: Cambridge, 2006.
(21) Curry, A.; Nusz, G.; Chilkoti, A.; Wax, A. *Opt. Express* **2005**, *13*, 2668–2677.
(22) Ruppin, R. *Surf. Sci.* **1983**, *127*, 108–118.
(23) Ruppin, R. *Physica A* **1991**, *178*, 195–205.
(24) Videen, G. *J. Opt. Soc. Am. A* **1992**, *9*, 844–845.
(25) Videen, G. *J. Opt. Soc. Am. A* **1991**, *8*, 483–489.
(26) Eremina, E.; Eremin, Y.; Wriedt, T. *Opt. Commun.* **2006**, *267*, 524–529.
(27) Malinsky, M. D.; Lance Kelly, K.; Schatz, G. C.; Van Duyne, R. P. *J. Phys. Chem. B* **2001**, *105*, 2343–2350.
(28) Oldenburg, S. J.; Averitt, R. D.; Westcott, S. L.; Halas, N. J. *Chem. Phys. Lett.* **1998**, *288*, 243–247.
(29) Brinson, B. E.; Lassiter, J. B.; Levin, C. S.; Bardhan, R.; Mirin, N.; Halas, N. J. *Langmuir* **2008**, *24*, 14166–14171.
(30) Nehl, C. L.; Grady, N. K.; Goodrich, G. P.; Tam, F.; Halas, N. J.; Hafner, J. H. *Nano Lett.* **2004**, *4*, 2355–2359.
(31) Lassiter, J. B.; Aizpurua, J.; Hernandez, L. I.; Brandl, D. W.; Romero, I.; Lal, S.; Hafner, J. H.; Nordlander, P.; Halas, N. J. *Nano Lett.* **2008**, *8*, 1212–1218.
(32) Johnson, P. B.; Christy, R. W. *Phys. Rev. B* **1972**, *6*, 4370–4379.
(33) Kvietkova, J.; Daniel, B.; Hetterich, M.; Schubert, M.; Spemann, D. *Thin Solid Films* **2004**, *455*, 228–230.
(34) Stratton, J. A. *Electromagnetic Theory*; McGraw-Hill: New York, 1941.

NL900945Q